Duplicated *P5CS* genes of Arabidopsis play distinct roles in stress regulation and developmental control of proline biosynthesis

Gyöngyi Székely[1], Edit Ábrahám[1], Ágnes Cséplő[1], Gábor Rigó[1], Laura Zsigmond[1], Jolán Csiszár[2], Ferhan Ayaydin[1], Nicolai Strizhov[3,†], Jan Jásik[3,4], Elmon Schmelzer[3], Csaba Koncz[1,3] and László Szabados[1,*]

[1]*Institute of Plant Biology, Biological Research Center, H-6726 Szeged, Hungary,*

[2]*Department of Plant Physiology, University of Szeged, H-6723 Szeged, Hungary, and*

[3]*Max-Planck-Institut für Züchtungsforschung, D-50829 Cologne, Germany, and*

[4]*Department of Plant Cell Biology, Institute of Cellular and Molecular Botany, University of Bonn, Kirschallee 1, D-53115 Bonn, Germany*

Summary

Δ-1-pyrroline-5-carboxylate synthetase enzymes, which catalyse the rate-limiting step of proline biosynthesis, are encoded by two closely related *P5CS* genes in Arabidopsis. Transcription of the *P5CS* genes is differentially regulated by drought, salinity and abscisic acid, suggesting that these genes play specific roles in the control of proline biosynthesis. Here we describe the genetic characterization of *p5cs* insertion mutants, which indicates that *P5CS1* is required for proline accumulation under osmotic stress. Knockout mutations of *P5CS1* result in the reduction of stress-induced proline synthesis, hypersensitivity to salt stress, and accumulation of reactive oxygen species. By contrast, *p5cs2* mutations cause embryo abortion during late stages of seed development. The desiccation sensitivity of *p5cs2* embryos does not reflect differential control of transcription, as both *P5CS* mRNAs are detectable throughout embryonic development. Cellular localization studies with *P5CS*–GFP gene fusions indicate that P5CS1 is sequestered into subcellular bodies in embryonic cells, where P5CS2 is dominantly cytoplasmic. Although proline feeding rescues the viability of mutant embryos, *p5cs2* seedlings undergo aberrant development and fail to produce fertile plants even when grown on proline. In seedlings, specific expression of P5CS2–GFP is seen in leaf primordia where P5CS1–GFP levels are very low, and P5CS2–GFP also shows a distinct cell-type-specific and subcellular localization pattern compared to P5CS1–GFP in root tips, leaves and flower organs. These data demonstrate that the Arabidopsis P5CS enzymes perform non-redundant functions, and that *P5CS1* is insufficient for compensation of developmental defects caused by inactivation of *P5CS2*.

Keywords: Δ-pyrroline-5-carboxylate synthase, regulation of proline biosynthesis, osmotic stress, localization of GFP fusion proteins, Arabidopsis, mutants.

Introduction

Proline accumulation is a common physiological response in higher plants exposed to drought and salinity (Delauney and Verma, 1993; Handa *et al.*, 1986). The positive effect of proline accumulation on osmotic stress tolerance was first observed in bacteria, with proline-over-producing strains showing enhanced salt tolerance (Csonka, 1981). Proline is considered to be an important osmolyte that acts as molecular chaperone stabilizing the structure of proteins, as

well as a regulator of cellular redox potential and an anti-oxidant controlling free radical levels (Hare *et al.*, 1999; Hong *et al.*, 2000). In higher plants, proline is synthesized from glutamate and ornithine, but the level of free proline is also controlled catabolically (Delauney and Verma, 1993; Nanjo *et al.*, 2003; Roosens *et al.*, 1998). Proline biosynthesis from glutamate is catalysed by a bifunctional Δ-1-pyrroline-5-carboxylate synthetase (P5CS) enzyme that yields pyrro-

line-5-carboxylate (P5C) in a two-step reaction (Hu *et al.*, 1992). The activity of P5CS represents a rate-limiting step in proline biosynthesis, which is controlled at the level of *P5CS* transcription and through feedback inhibition of P5CS by proline (Savouré *et al.*, 1995; Strizhov *et al.*, 1997; Yoshiba *et al.*, 1995; Zhang *et al.*, 1995). P5C is further reduced to proline by the 1-pyrroline-5-carboxylate reductase (P5CR) enzyme (Delauney and Verma, 1990; Rayapati *et al.*, 1989; Verbruggen *et al.*, 1993). In the catabolic pathway, proline is oxidized to glutamate in mitochondria through reduction of proline to P5C by proline dehydrogenase (PDH) (Peng *et al.*, 1996; Verbruggen *et al.*, 1996), and subsequent oxidation of P5C to glutamate by P5C dehydrogenase (P5CDH) (Deuschle *et al.*, 2001; Forlani *et al.*, 1997). Reciprocal regulation of *P5CS* and *PDH* genes plays a key role in the control of proline levels during and after osmotic stress (Kiyosue *et al.*, 1996).

To clarify the physiological role of proline in various stress responses, both proline biosynthetic and catabolic pathways have been modified in transgenic plants. Proline-over-producing plants were obtained by over-expression of *P5CS* genes (Kishor *et al.*, 1995) and reduction of feedback inhibition of P5CS enzymes by proline (Hong *et al.*, 2000; Zhang *et al.*, 1995). Alternatively, proline accumulation was achieved by T-DNA tagging of the *PDH* gene and antisense inhibition of *PDH* transcription (Mani *et al.*, 2002; Nanjo *et al.*, 2003). In some reports, an increased level of free proline was found to correlate with improved stress tolerance (Hong *et al.*, 2000), whereas in others such a correlation was not apparent (Mani *et al.*, 2002). Down-regulation of proline biosynthesis by antisense inhibition of *P5CS* is reported to reduce free proline content and cause developmental alterations and elevated stress sensitivity in Arabidopsis (Nanjo *et al.*, 1999). However, P5CS is encoded by two closely related genes in Arabidopsis, and it is not yet known how antisense approaches affect the function of the individual *P5CS* homologues. Although many physiological studies have suggested that proline is implicated in multiple stress protection mechanisms, it is also apparent that proline accumulation does not represent an exclusive condition for mounting stress tolerance responses. Thus, several salt- and cold-hypersensitive Arabidopsis mutants accumulate proline at high levels without any apparent beneficial effect on stress tolerance (Liu and Zhu, 1997). In *pdh* mutants and plants expressing antisense *PDH* constructs, impaired proline degradation results in severe toxicity (Mani *et al.*, 2002; Nanjo *et al.*, 2003). Therefore, how proline accumulation influences particular regulatory pathways in complex stress responses is still a matter of debate (Maggio *et al.*, 2002).

Previous studies revealed characteristic differences in transcriptional control of the closely related *P5CS* genes in Arabidopsis. Transcription of the *P5CS1* gene is inducible by salt, drought, glucose and sucrose treatments in an abscisic

acid (ABA)- and light-dependent fashion (Ábrahám *et al.*, 2003; Strizhov *et al.*, 1997). Steady-state *P5CS1* transcript levels are significantly higher in most plant organs compared to those of *P5CS2*, which appears to be preferentially expressed in dividing cells and in response to incompatible pathogenic interactions (Fabro *et al.*, 2004; Strizhov *et al.*, 1997). To determine the extent of functional diversification of duplicated *P5CS* genes in the developmental and stress-dependent control of proline biosynthesis, we describe here the genetic and physiological characterization of Arabidopsis *p5cs1* and *p5cs2* T-DNA insertion mutants.

Results

Characterization of p5cs1 *mutants*

We have characterized four *p5cs1* insertion mutations obtained from the SALK collection (Figure 1a) (Alonso *et al.*, 2003). The SALK_058000 mutant (*p5cs1-1*) carries a T-DNA insertion in *P5CS1* sequences representing the 5′ UTR of the mRNA, 160 bp upstream of the ATG codon. In the SALK_045245 (*p5cs1-2*) and SALK_037850 (*p5cs1-3*) mutants, the T-DNA insertions are localized 107 and 718 bp downstream of the ATG in introns 1 and 3, respectively. In the SALK_063517 line (*p5cs1-4*), the T-DNA insertion is localized 3208 bp downstream of ATG in exon 14 (see also Appendix S1). Transcription of the *p5cs* mutant alleles was characterized by semi-quantitative RT-PCR using RNA templates isolated from 2-week-old seedlings grown either without salt or in the presence of 200 mM NaCl for 24 h. Using a primer pair for amplification of the full-length cDNA, a residual low level of *P5CS1* transcription was detected in the salt-treated *p5cs1-1* and *p5cs1-3* mutants that carried T-DNA insertions in the 5′ leader region and intron 3, respectively. The levels of full-length transcripts in the *p5cs1-1* and *p5cs1-3* mutants were 2 and 6%, respectively, of the *P5CS1* RNA level in the salt-treated wild-type control, indicating that these lines represent strong knock-down alleles (Figure 1b).

Because all SALK T-DNA insertions carry a CaMV 35S promoter upstream of the T-DNA left border that drives transcription through the insert junctions, we also examined whether *P5CS1* sequences located downstream of the various insertions are transcribed in the mutants. RT-PCR amplification of 3′ UTR region of *P5CS1* (Figure 1b, primers p5c1A+B) detected less than 2% transcript in the *p5cs1-1* mutant and an even lower level of truncated *P5CS1* RNA in the *p5cs1-4* knockout line. By contrast, levels of truncated *P5CS1* mRNAs that were 25–35% of those of the salt-treated wild-type control were found in the *p5cs1-2* and *p5cs1-3* mutants in both the presence and absence of salt induction, indicating that the bulk of these truncated RNAs are transcribed from the CaMV 35S promoter. These data suggest that the *p5cs1-2* and *p5cs1-3* mutations allow the

Figure 1. Characterization of *p5cs1* insertion mutants.

(a) Positions of T-DNA insertions in the *P5CS1* gene. Four *p5cs1* SALK T-DNA insertion alleles were identified: *p5cs1-1* (5′ UTR), *p5cs1-2* (intron 1), *p5cs1-3* (intron 3), and *p5cs1-4* (exon 14). Arrows show the positions of PCR primers used in RT-PCR analysis.

(b) Semi-quantitative RT-PCR analysis of transcription of *p5cs1* alleles using RNA templates isolated from 2-week-old wild-type (Col-0) and *p5cs1* seedlings grown either in 0.5 MS medium or subjected to treatment with 200 mm NaCl for 24 h.

(c) Comparison of proline levels in wild-type and *p5cs1* mutant plants. Proline was measured in leaves and flowers of 6-week-old plants grown under optimal conditions in soil. FW, fresh weight.

(d) Proline content in 3-week-old seedlings treated with 200 mm NaCl for 48 h. Control: seedlings without salt treatment.

(e) Effect of drought on proline accumulation in *p5cs1* and wild-type plants after 10 days of water deprivation (i.e. 80% decrease in soil water content).

(f) Relative water content (RWC) of wild-type and *p5cs1* plants before and after drought treatment. Error bars indicate standard deviations of the means of at least three experiments. Values marked by different letters show significant differences between the treatments ($P < 0.05$, Duncan test).
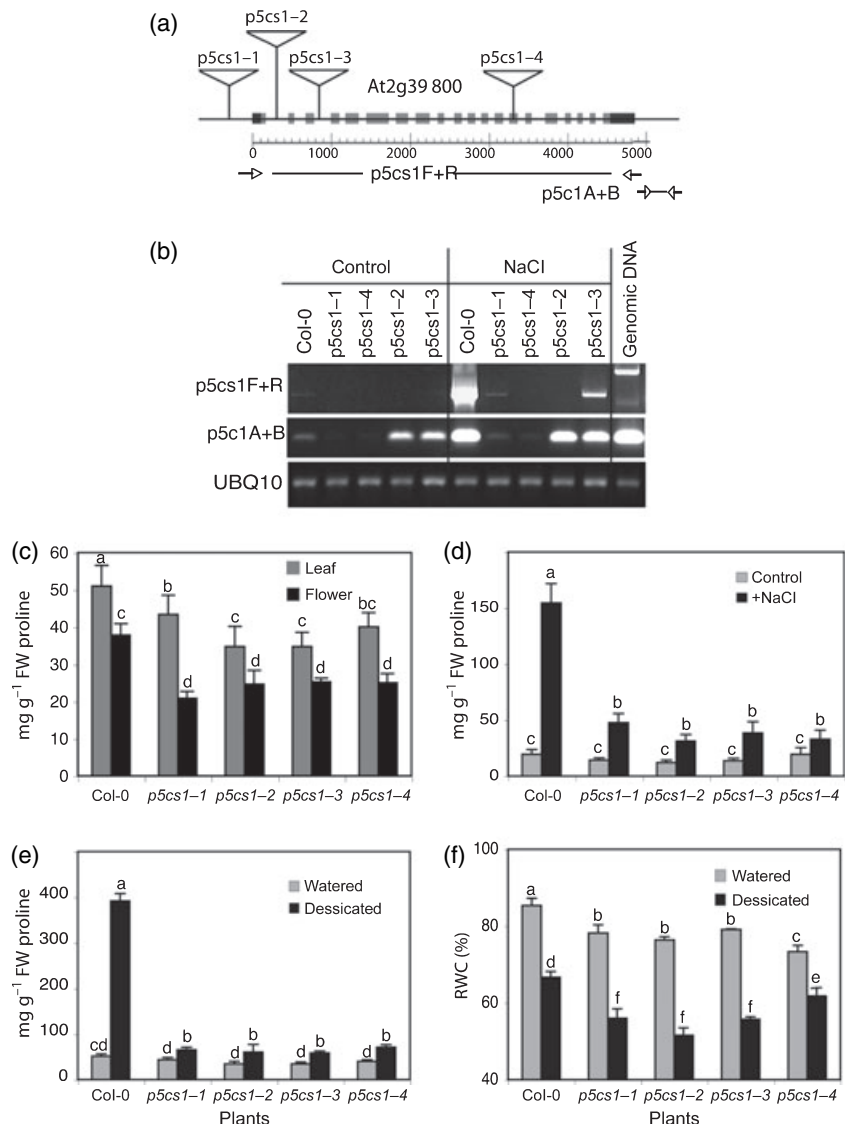
synthesis of truncated P5CS1 enzymes that lack the N-terminal γ-glutamyl kinase domain. Because the γ-glutamyl kinase activity is absolutely essential for the first step of proline biosynthesis, both the *p5cs1-2* and *p5cs1-3* mutations affected proline biosynthesis analogously to the strong knock-down allele *p5cs1-1* and the *p5cs1-4* null mutation, which inactivated the C-terminal glutamic-γ-semi-aldehyde dehydrogenase domain.

Stress-induced proline accumulation is compromised in the p5cs1 mutants

Under standard growth conditions, all *p5cs1* mutants showed wild-type development in both soil and sterile culture. In rosette leaves of 6-week-old soil-grown *p5cs1* plants, the free proline content was 15–30% lower compared to wild-type, whereas in flowers this difference was 35–45% (Figure 1c). The observed decrease in proline content of

p5cs1 mutants indicated the contribution of P5CS1 to proline synthesis under normal growth conditions in sterile culture, and showed that P5CS2 maintains a sufficiently high level proline biosynthesis without limiting growth and fertility. To determine the effects of *p5cs1* mutations on salt-induced proline accumulation, *in vitro*-cultured 3-week-old wild-type and *p5cs1* seedlings were exposed to 200 mm NaCl treatment for 48 h (Figure 1d). Compared to untreated controls, the free proline levels increased sevenfold in wild-type during salt treatment, but only two- to threefold in the *p5cs1* mutants. This striking difference clearly shows that the deficiency of P5CS1 was not fully compensated by *P5CS2*, and indicates that *P5CS1* plays a critical role in the regulation of proline accumulation during salt stress.

To examine how changes in proline accumulation correlate with alterations in water relations, wild-type and *p5cs1* plants were exposed to drought treatment by stopping irrigation for 10 days. While soil humidity decreased from

60% to 10% during this period, the concentration of free proline in the rosette leaves of wild-type plants increased up to eightfold, compared to an increase of no more than twofold in the *p5cs1* mutants (Figure 1e). This indicated that, similarly to salt stress, *P5CS1* also plays a key role in drought-induced accumulation of proline. The drought treatment used resulted in a reduction of relative water content (RWC) from 85% to 67% in wild-type plants, compared to a decrease in RWC from 74–78% to 50–60% in the *p5cs1* mutants (Figure 1f). The greater than fivefold reduction of proline accumulation thus correlated with a decrease in RWC of only 10–15% in the *p5cs1* mutants. The fact that water loss in detached leaves was similar in wild-type and *p5cs1* mutants (data not shown) supported the conclusion that proline accumulation is not a critical factor in complex control of RWC.

p5cs1 *mutations result in reduced salt tolerance*

To assess the effects of *p5cs1* mutations on plant growth under salt stress, we performed comparative assays of germination, root elongation, seedling growth and induction of chlorosis using wild-type and *p5cs1* plants grown either in the absence or presence of 150 or 200 mM NaCl. Germination rates of wild-type and *p5cs1* seeds were similar under all conditions tested (data not shown), indicating that *P5CS1* plays no role in the control of seed germination. Whereas root elongation rates of wild-type and *p5cs1* seedlings were comparable without salt treatment, the *p5cs1* mutants displayed 25% and 50% reduction of root growth rate compared to wild-type in the presence of 150 and 200 mM NaCl, respectively (Figure 2a,b). The *p5cs1* mutants also displayed lower salt tolerance in other assays monitoring leaf development, fresh weight accumulation and plant survival (data not shown).

Enhanced bleaching and subsequent death of *p5cs1* mutants was observed in the presence of 200 mM NaCl, which affected but did not prevent the growth and survival of wild-type seedlings (Figure 2c). Induction of leaf chlorosis in the salt-treated *p5cs1* mutants suggested an increase of oxidative damage by enhanced generation of reactive oxygen species (ROS). Hence, we compared ROS levels in leaves of salt-treated wild-type and *p5cs1* plants using a histochemical assay with 3,3′-diaminobenzidine (DAB). Leaves of wild-type and *p5cs1* mutant plants grown without salt showed comparable levels of DAB staining in vascular tissues. Upon 24 h exposure to 150 mM NaCl, DAB-staining was also detected in mesophyll tissues of leaf blades and showed higher intensity in the *p5cs1* mutants than in wild-type, indicating enhanced hydrogen peroxide accumulation (Figure 2d).

To confirm that salt hypersensitivity of *p5cs1* mutants indeed reflected insufficient proline accumulation, we measured the salt-mediated inhibition of root elongation of *p5cs1* mutants grown in either the absence or presence of externally provided proline. Remarkably, addition of 10 mM proline to the medium alleviated the salt-dependent root growth defects of *p5cs1* mutants (Figure 2e), indicating a causal relationship between reduced salt tolerance and impaired proline accumulation. To prove unequivocally that the salt hypersensitivity phenotype was caused by the *p5cs1* mutations, we performed genetic complementation assays. The coding sequence of green fluorescent protein (GFP) was inserted into the wild-type *P5CS1* gene by precisely replacing its stop codon (Figure S1), and the resulting *P5CS1*–GFP reporter gene was introduced by the *Agrobacterium* binary vector pPCV812 into the homozygous *p5cs1* mutants. Salt-dependent proline accumulation in the GFP-expressing *p5cs1* mutants reached 80–90% of control wild-type levels (Figure 2f). The salt sensitivity of genetically complemented homozygous *p5cs1* mutants (shown for *p5cs1-4* in Figure 2g) was similar to that of wild-type, indicating correct regulation of the *P5CS1*–GFP construct.

Enhancement of oxidative damage in the p5cs1 *mutants*

In comparison to wild-type, prolonged salt stress led to enhanced chlorosis of *p5cs1* mutants. Whereas total leaf chlorophyll contents of wild-type and *p5cs1* plants were similar on salt-free medium, the chlorophyll content following 24 h treatment with 150 mM NaCl was reduced by 15–20% in wild-type compared to a 30–40% reduction in *p5cs1* plants. Treatment with 200 mM NaCl decreased the chlorophyll content by 30% in wild-type compared to a 50–60% reduction in *p5cs1* plants (Figure 3a). The significant increase in chlorophyll degradation provided an indication of enhanced oxidative damage in the salt-stressed *p5cs1* mutants. Quantitative measurement of DAB reactions in leaves indicated an increase in hydrogen peroxide accumulation of about twofold in the *p5cs1* mutants compared to wild-type in response to treatment with 200 mM NaCl for 24 h (Figure 3b). Because lipid peroxidation is a direct consequence of ROS accumulation, we monitored the levels of malonaldehyde (i.e. the end product of lipid peroxidation) in leaves of control and salt-treated plants. Lipid peroxidation was similar in non-stressed *p5cs1* and wild-type, and did not increase significantly in salt-stressed wild-type plants. However, in the *p5cs1* mutants, malonaldehyde levels were twofold higher than in wild-type plants upon 24 h treatment with 200 mM NaCl (Figure 3c), correlating with the observed increase in hydrogen peroxide levels. Enhancement of lipid peroxidation suggests considerable oxidative membrane damage during stress in the *p5cs1* mutants.

ROS levels are controlled by a well-defined detoxification system, which involves a number of enzymes that reduce the amount of reactive oxygen species. To monitor ROS detoxification, the activities of catalase (CAT), superoxide dismutase (SOD), glutathione-*S*-transferase (GST), glutathi-

Figure 2. Sensitivity of wild-type and *p5cs1* plants to salt stress.

(a) Five-day-old seedlings were transferred onto vertical 0.5 MS agar plates containing either no salt, or 150 or 200 mM NaCl. Growth was monitored for 16 days.

(b) Root elongation rates in response to salt stress. Root elongation was registered daily between days 5 and 21 after transferring seedlings to salt-free and NaCl-containing media.

(c) Survival of wild-type and *p5cs1-1* seedlings on high-salt medium. Five-day-old seedlings were transferred to 0.5 MS medium containing 200 mM NaCl, and survival was monitored at weekly intervals. Wild-type and *p5cs1-1* seedlings are shown after 3 weeks of salt-treatment. All four *p5cs1* mutants displayed similar survival rates (not shown).

(d) Detection of ROS by DAB reaction in leaves of wild-type and *p5cs1* plants exposed to 200 mM NaCl treatment for 24 h before performing the assay.

(e) Complementation of salt hypersensitivity of the *p5cs1-1* mutant by proline. Wild-type and *p5cs1-1* seedlings were grown for 3 weeks on 0.5 MS medium supplemented with 150 mM NaCl in the absence or presence of 10 mM proline. All other *p5cs1* mutants showed similar responses (data not shown).

(f, g) Complementation of *p5cs1-4* mutant with the *P5CS1*–GFP gene construct. (f) Proline accumulation in wild-type, *p5cs1-4* and genetically complemented *p5cs1-4* mutant plants after exposing them to 200 mM NaCl stress for 36 h. Different letters show a significant difference between the treatments ($P < 0.05$, Duncan test).

(g) Growth and survival of wild-type, *p5cs1-4* and complemented *p5cs1-4* mutant plants cultured on 200 mM NaCl-containing medium for 3 weeks.
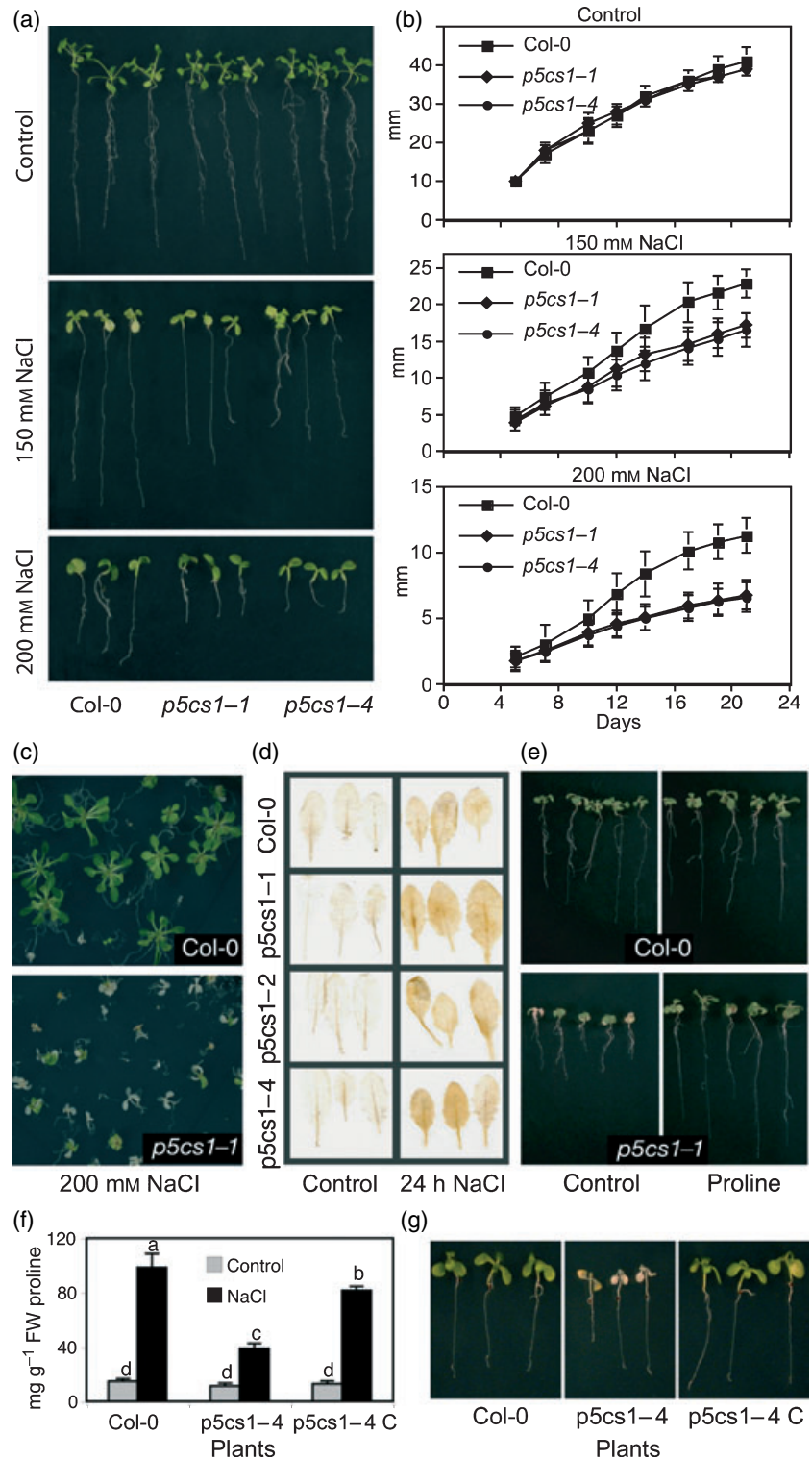
one reductase (GR), ascorbate peroxidase (APX) and guaiacol peroxidase (GPX) were measured in leaves of wild-type and *p5cs1* plants that were subjected to 200 mM NaCl treatment for 24 h in hydroponic cultures. Catalase eliminates hydrogen peroxide and is one of the most important detoxifying enzymes during oxidative stress. On average, an 80–120% increase in catalase activity was detected in the *p5cs1* mutants compared to a 40% increase in wild-type during salt stress (Figure 4a). GPX activities showed only marginal enhancement in the mutants (Figure 4b), whereas
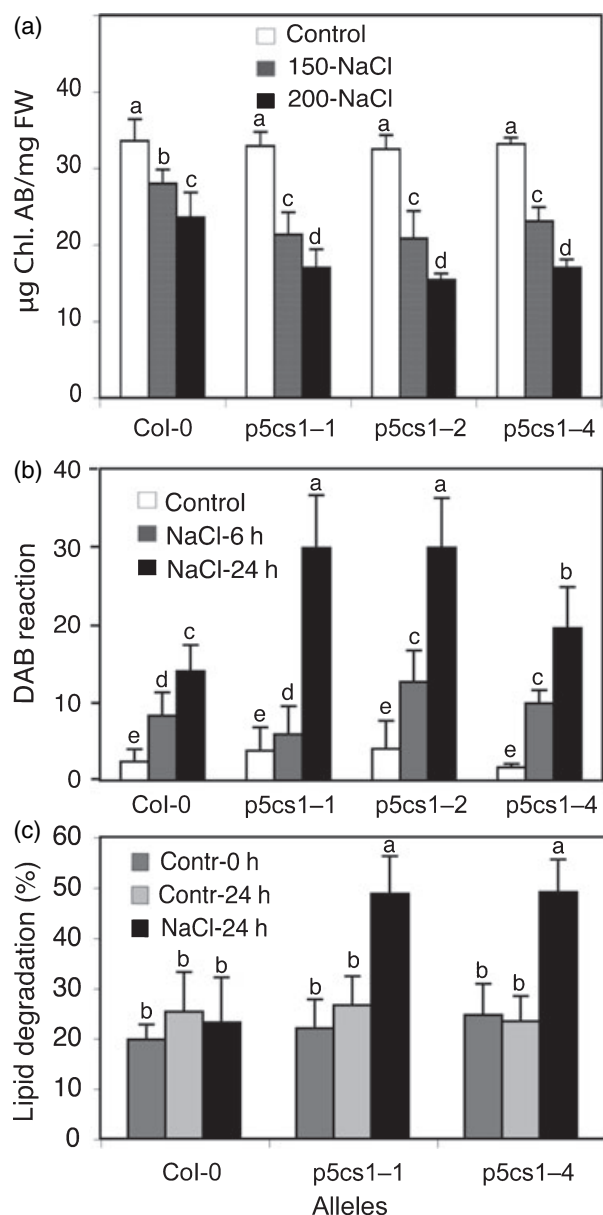
Figure 3. Oxidative damage in the *p5cs1* mutants.

(a) Comparison of chlorophyll contents of wild-type and *p5cs1* seedlings upon transfer to 0.5 MS medium containing no salt (control), or 150 or 200 mM NaCl.

(b) Quantitative analysis of the DAB reaction in salt-stressed leaves. NaCl (200 mM) was applied for either 6 or 24 h, and the DAB assay was performed on 20 leaves of wild-type and *p5cs1* mutants. Control: leaves without salt treatment.

(c) Lipid peroxidation rates in leaves of wild-type, *p5cs1-1* and *p5cs1-4* plants, treated as described in (b). Values show the ratio of degraded lipids as determined by measuring MDA production. All experiments were performed with 20 plants in three independent replicates. Values marked by different letters show a significant difference between the treatments ($P < 0.05$, Duncan test).

SOD activities, mediating the reduction of superoxide radicals to hydrogen peroxide, were slightly reduced in *p5cs1* plants (Figure 4c). The GST, GR and APX enzymes, which act in the stress-regulated glutathione–ascorbate cycle showed 40–60% higher activities in wild-type, compared to an increase of only 10–20% in the salt-treated *p5cs1* mutants, indicating that this detoxifying pathway did not function to such an extent in the mutants (Figure 4d–f). Control Northern hybridizations did not reveal alterations in transcript levels of *CAT2* and *APX* genes in the *p5cs1* mutants (data not shown), suggesting that the observed changes in these enzyme activities did not reflect alterations at the level of transcription.

Knockout mutations in the P5CS2 gene cause embryo lethality

To determine the effects of *P5CS2* knockout mutations, we have characterized two *p5cs2* (At3g55610) alleles identified in the GABI-KAT and FLAG insertion mutant collections (Figure 5a). The *p5cs2-1* allele (GABI_452G01) carries a single T-DNA insertion in intron 18 (4063 bp downstream of ATG), whereas the *p5cs2-2* allele (FLAG_139H07) contains a T-DNA tag disrupting exon 2 (804 bp downstream of ATG; see Appendix S1). PCR screening for homozygous lines in the segregating T_2 and T_3 mutant families failed to identify homozygous *p5cs2-1* and *p5cs2-2* progeny. In the presence of sulfadiazine (GABI line) or kanamycin (FLAG line), the hemizygous T_3 families showed 2:1 segregation of resistant versus sensitive seedlings. Inspection of siliques of hemizygous *p5cs2-1* and *p5cs2-2* mutants revealed 3:1 segregation of wild-type and collapsed seeds (Figure 5b). In immature green siliques, a similar segregation of green and white seeds was observed. Between days 7 and 10 after pollination, depending on the humidity levels, all white seeds collapsed and turned brown rapidly (Figure 5c). Examination of cleared seeds revealed that embryo development was considerably delayed in white mutant seeds. After reaching either torpedo stage at 40–50% humidity or U-shape stage at 70–80% humidity, the embryos in white seeds of both *p5cs2* insertion mutants ceased growing and aborted (Figure 5d,e).

When dissected aseptically and cultured in the presence of 10 mM proline, both green and white seeds germinated to viable seedlings. In the absence of proline, however, white seeds either did not germinate or produced arrested white seedlings. About 30% of seedlings derived from white seeds germinating in the presence of proline displayed developmental abnormalities, such as aberrantly shaped cotyledons and leaves (Figure 5f). PCR genotyping revealed that seedlings obtained from white seeds were homozygous for the *p5cs2-1* and *p5cs2-2* mutations, whereas seedlings from green seeds corresponded to either hemizygous or wild-type progeny (Figure 5g). RT-PCR analysis of RNA templates isolated from single leaves of homozygous *p5cs2-1* and *p5cs2-2* seedlings did not detect *P5CS2* transcript (Figure 5h), indicating that T-DNA insertions in both exon 2

Figure 4. Activity of detoxifying enzymes in wild-type and *p5cs1* mutants.

Six-week-old plants were treated with 200 mM NaCl for 24 h in hydroponic cultures followed by measurement of (a) catalase (CAT), (b) guayacol peroxidase (GPX), (c) superoxide dismutase (SOD), (d) ascorbate peroxidase (APX), (e) glutathione-S-transferase (GST), and (f) glutathione reductase (GR) enzyme activities in leaves collected from 10 plants in three independent experiments. Means marked by different letters show a significant difference between the treatments ($P < 0.05$, Duncan test).
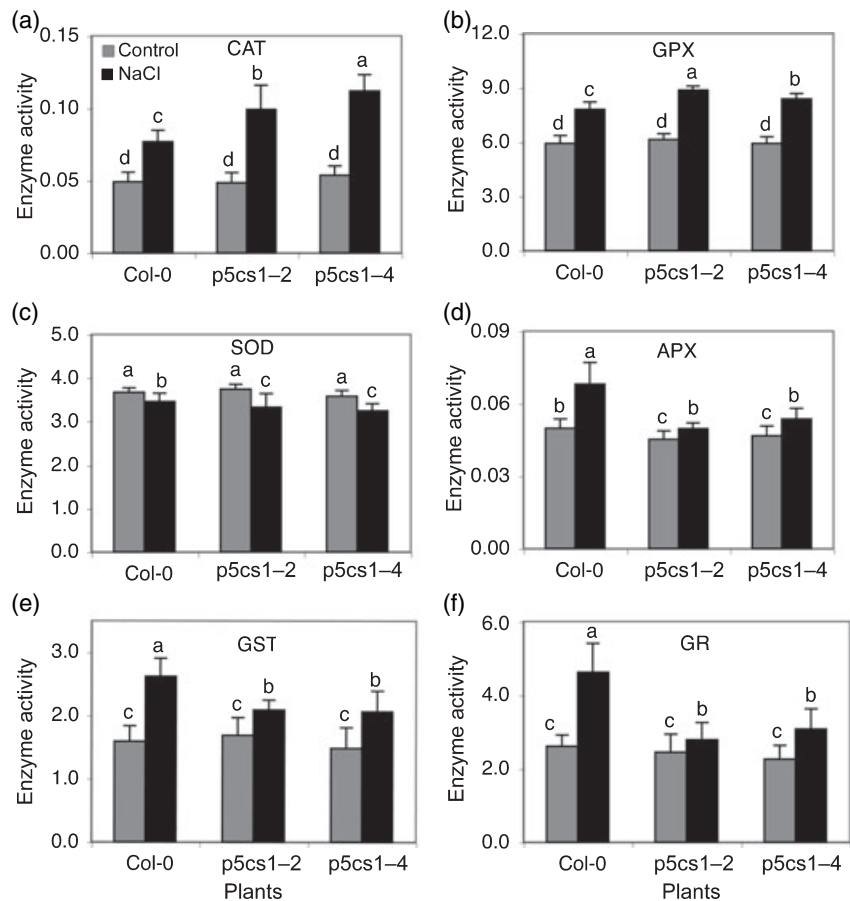
and intron 16 caused null mutations of the *P5CS2* gene. The embryo-lethal phenotype of these mutations suggests that the loss of *P5CS2* function results in proline auxotrophy during embryogenesis. The *p5cs2* mutations also affected plant development after germination. When grown on proline-containing medium, the mutants showed extremely slow growth, and upon transfer into soil they grew as dwarfs with aberrant rosettes for 1–2 weeks, but ultimately decayed even when treated with proline under optimal growth conditions.

As described for the *p5cs1* mutants, we also performed genetic complementation of the *p5cs2-1* mutation with a *P5CS2*–GFP reporter gene. Hemizygous *p5cs2-1/+* plants were transformed with *Agrobacterium* vector pPCV812 carrying a *P5CS2* gene in which the stop codon was replaced with a precise fusion of GFP coding sequences (see Experimental procedures and Figure S1). T_2 families of transformed lines were screened for GFP expression and segregation of homozygous *p5cs2* mutant plants (Figure 5). The genetic complementation tests yielded homozygous *p5cs2-1* lines expressing the P5CS2–GFP protein, and the phenotype and viability of these lines were similar to wild-type plants. This result confirmed that the *p5cs2-1* mutation was indeed responsible for the observed embryo and

seedling lethality traits, and indicated that the P5CS2–GFP protein conferred restoration of the mutant to the wild-type phenotype. Interestingly, in one of the transformed families (P5CS2–GFP/5), all T_2 offspring were homozygous for the *p5cs2-1* mutation (Figure 5i), suggesting that *Agrobacterium* transformation took place before fertilization of the mutant ovule with a mutant pollen, generating a complemented homozygous embryo.

Differences in spatial distribution and subcellular localization of P5CS enzymes

Although the observed effects of *p5cs1* mutations were consistent with the previously suggested regulatory role of P5CS1 in stress-induced proline synthesis, the lethality of the *p5cs2* mutations predicted that P5CS2 might have a distinct function in embryo and seedling development. However, neither hybridization analyses of the organ-specific distribution of *P5CS* transcripts nor studies of spatial and temporal expression patterns of *P5CS* promoter–GUS reporter fusions provided sufficiently high resolution to confirm this model (Ábrahám *et al.*, 2003). Therefore, we performed *in situ* hybridizations of embryo sections using gene-specific probes. These experiments revealed the
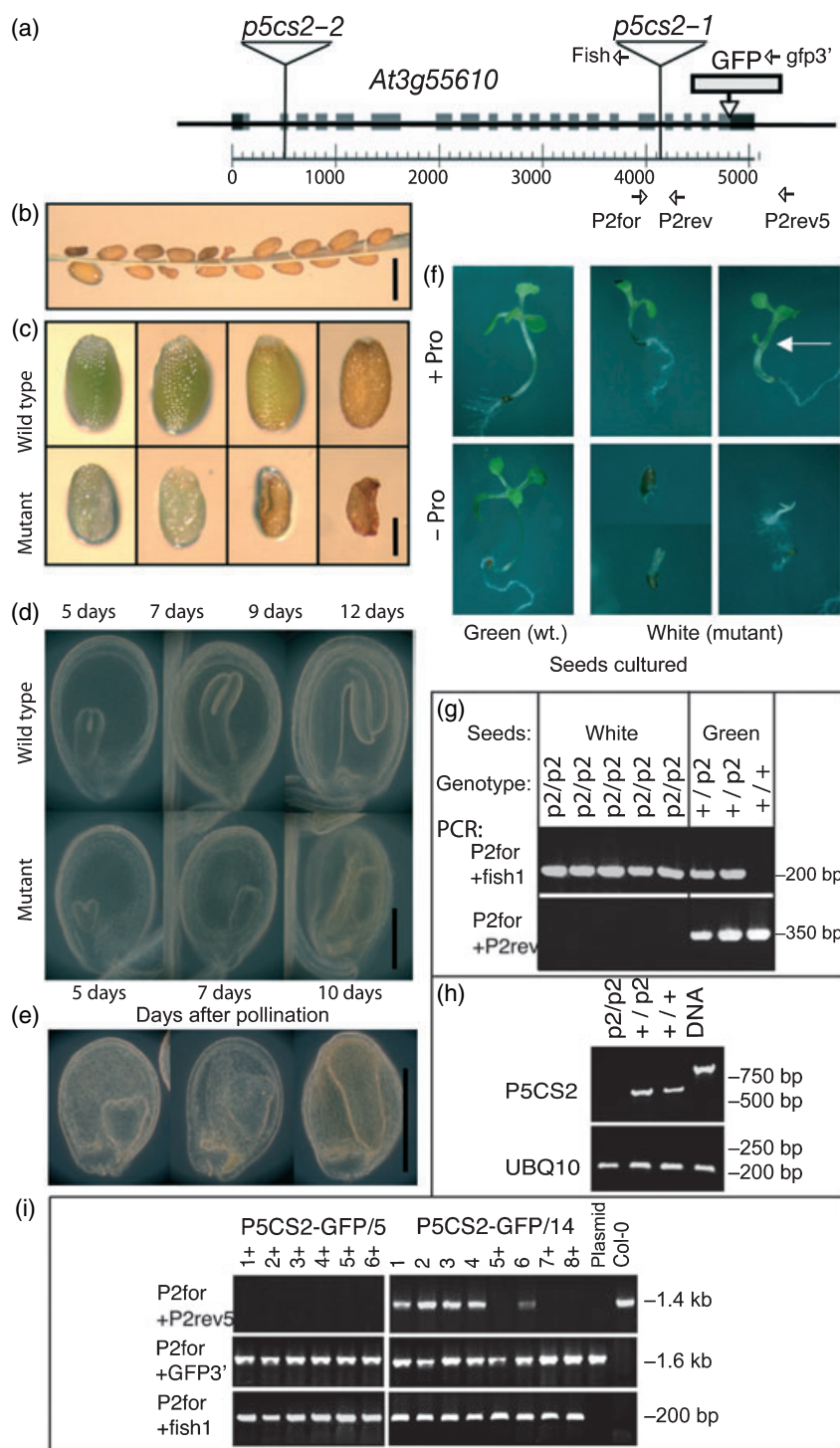
Figure 5. The *p5cs2* mutations cause embryo lethality.

(a) T-DNA insertions in the *P5CS2* gene (At3g55610) were localized in intron 16 (*p5cs2-1*) and exon 2 (*p5cs2-2*). The positions of primers (P2for, P2rev, P2rev5, fish1, gfp3′) used for PCR analysis are indicated.

(b) Mature silique of a hemizygous *p5cs2-1* plant containing wild-type and aborted mutant seeds (bar = 1 mm).

(c) Development of wild-type and mutant seeds in *p5cs2-1/+* siliques. In contrast to wild-type seeds, homozygous *p5cs2-1* mutant seeds turned white and aborted 7 days after pollination (bar = 0.2 mm).

(d) Development of wild-type and *p5cs2-1* embryos in *p5cs2-1/+* siliques under 50% humidity. Top row: early-torpedo, late-torpedo and U-shape stage embryos in wild-type seeds. Bottom row: seeds with delayed heart, torpedo stage and collapsed U-shape stage *p5cs2-1* embryos (bar = 200 μm).

(e) Development of *p5cs2-2* embryos in siliques of plants grown in the presence of 70% humidity (bar = 200 μm).

(f) Rescue of *p5cs2-1* mutant by proline. Wild-type (green) and mutant (white) seeds were excised from green *p5cs2-1/+* siliques and cultured in either the absence (−Pro) or presence (+Pro) of 10 mM proline. The arrow indicates an aberrant mutant seedling with an extra leaf initial emerging from the hypocotyl.

(g) PCR genotyping for homozygous (p2/p2), heterozygous (+/p2) and wild-type (+/+) seedlings. The T-DNA insertion was detected with a combination of gene-specific (P2for) and T-DNA-specific (fish1) primers, and the wild-type *P5CS2* allele was amplified with gene-specific primers P2for and P2rev.

(h) RT-PCR analysis of *P5CS2* RNA with primers P2for and P2rev in homozygous (p2/p2), heterozygous (+/p2) and wild-type (+/+) seedlings. Control PCR reactions were performed with primers for ubiquitin 10 (UBQ10) and genomic DNA (DNA).

(i) Genetic complementation of *p5cs2-1* mutant with the *P5CS2*–GFP construct. Sulfadiazine-resistant T₂ seedlings were tested for the presence of the wild-type *P5CS2* gene (P2for+-P2rev5), the *P5CS2*–GFP gene fusion (P2for+GFP3′) and the T-DNA insertion (P2for+-fish1) using gene-, T-DNA- and GFP-specific primers. Complemented homozygous *p5cs2-1* mutants (marked +) carry the 1.6kb *P5CS2*–GFP fragment and a 200 bp T-DNA tag-specific fragment, but lack the 1.4 kb fragment of the wild-type gene. The P5CS2–GFP/5 line is homozygous, while the P5CS2–GFP/14 line is heterozygous, where the *p5cs2-1* mutation is segregating.

presence of both *P5CS1* and *P5CS2* transcripts during all stages of embryogenesis (Figure 6a,b). Because all hybridizations were performed under identical conditions, differences in signal intensity indicated that the levels of *P5CS1* transcript compared to *P5CS2* were somewhat higher throughout embryo development, especially in heart and torpedo stages. Thus, abortion of *p5cs2* mutant embryos could not be explained by down-regulation of *P5CS1* transcription during embryogenesis.

Monitoring temporal and spatial expression patterns of the *P5CS1*–GFP and *P5CS2*–GFP constructs, in which the translation stop codons of *P5CS* genes were replaced by coding sequences of enhanced GFP (eGFP), demonstrated that both P5CS–GFP proteins were synthesized at all stages

Figure 6. *P5CS1* and *P5CS2* expression in developing embryos.

(a, b) From left to right: *in situ* hybridization of wild-type globular, heart, torpedo and U-shaped embryos with *P5CS1*- (a) and *P5CS2*-specific (b) hybridization probes (bars = 100 μm).

(c–f) Detection of P5CS1–GFP (c,d) and P5CS2–GFP (e,f) proteins in heart and late-torpedo embryos by laser scanning confocal microscopy (bars = 50 μm).

(g–j) Subcellular localization of P5CS1–GFP protein in embryos. (g) Light image; (h) GFP fluorescence (note dotted pattern); (i) labelling of mitochondria with MitoTracker (Invitrogen; http://www.invitrogen.com); (j) red chlorophyll-derived fluorescence of chloroplasts.

(k) Enlarged image of (j) with overlay of images (h) and (i). The higher resolution of framed image sections in (k1) to (k4) shows lack of co-localization of P5CS1–GFP with mitochondria (yellow fluorescence) and chloroplasts (red fluorescence). Bars = 5 μm (g–k, k1–k4).
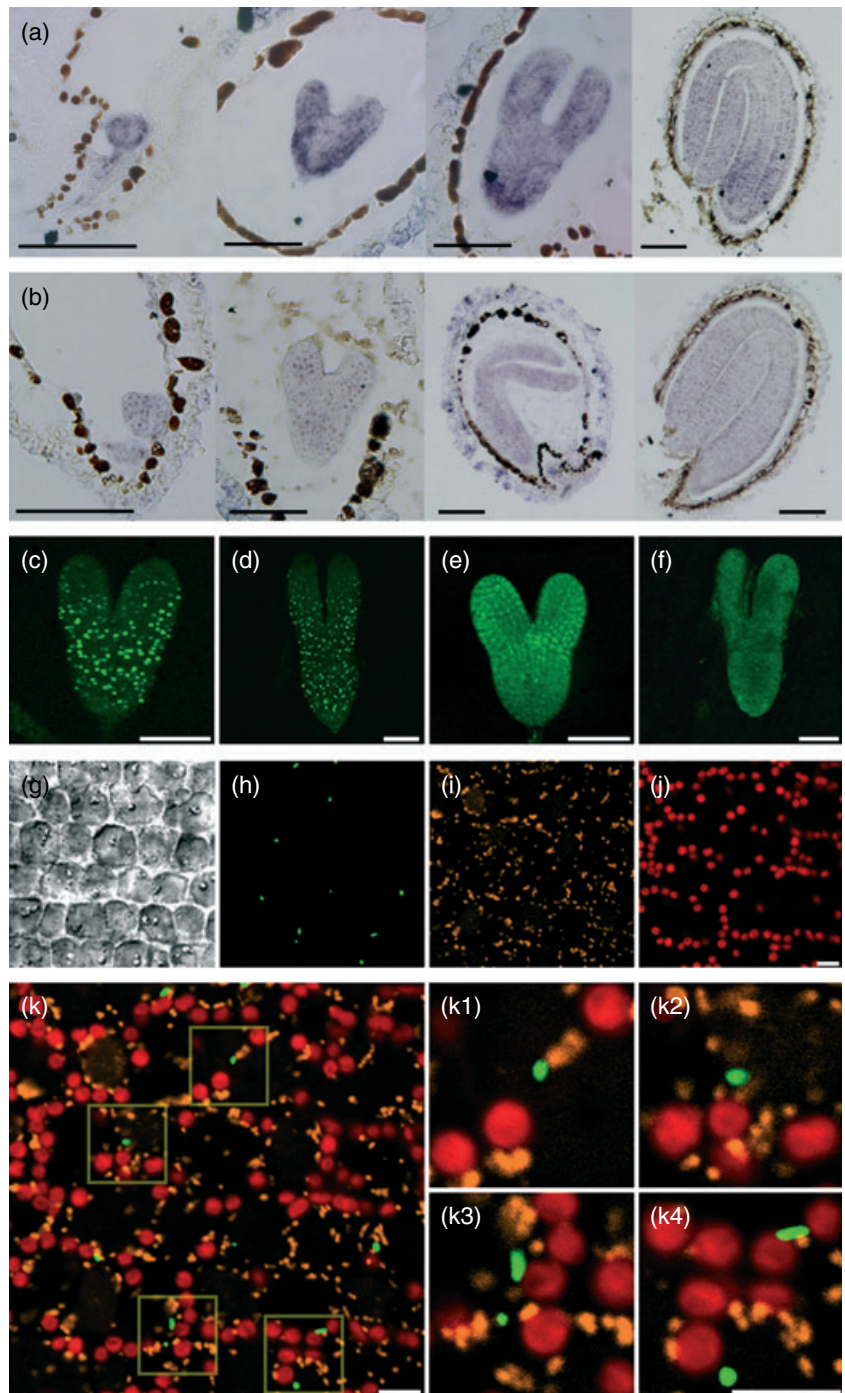
of embryogenesis. However, P5CS1–GFP displayed a remarkable dotted pattern in embryonic cells (Figure 6c,d), contrasting with the homogeneous cytoplasmic distribution of P5CS2–GFP (Figure 6e,f). High-resolution confocal laser scanning microscopy revealed that P5CS1–GFP was sequestered into subcellular bodies, which showed no co-localization with chloroplasts, mitochondria or nuclei (Figure 6g–k). The P5CS1 and P5CS2 proteins share 89% sequence identity, but none of the regions with amino acid exchanges were found to correspond to known secretion and sorting signals using various signal peptide predicting programmes (see Experimental procedures). Our experiments also excluded artificial vesicular targeting of P5CS1–GFP, because both P5CS–GFP gene fusions were generated by preserving all native transcription and translation regulatory elements.

The aberrant leaf and rosette development of proline-rescued *p5cs2* mutant seedlings suggested that the *p5cs2* mutations also affect later stages of plant development.

Therefore, we characterized spatial regulation of P5CS–GFP reporter constructs throughout the entire life cycle. In 5-day-old seedlings, only very low levels of P5CS1–GFP were observed in the cotyledons and hypocotyls. By contrast, P5CS2–GFP expression was detected in all seedling organs, at particularly high levels in shoot tips, and in vascular tissues of cotyledons and hypocotyls (Figure 7a). Remarkably, P5CS2–GFP appeared to be a specific early marker for leaf primordia in the apical meristems of seedlings (Figure 7b,c) and auxiliary leaf buds of rosettes (Figure 7d), in which P5CS1–GFP was not expressed. In inflorescence meristems, flower primordia and flower buds, P5CS2–GFP expression generally exceeded the levels of P5CS1–GFP (Figure 7e). In flowers, P5CS1–GFP was present only in anthers, while P5CS2–GFP expression could also be detected in anthers, stamen filaments, sepals and petals (Figure 7f). P5CS1–GFP showed specific expression in tissue layers carrying pollen mother cells in the stamens, as well as in pollen grains. In comparison, P5CS2–GFP was only expressed in the vegetative cells of stamens (Figure 7g,h).

In whole-mount roots, confocal imaging of P5CS1–GFP detected only dotted patterns of subcellular bodies, whereas P5CS2–GFP showed cytoplasmic localization accompanied by the appearance of some dots in few cells of the root elongation zone (Figure 7i,k). In response to treatment of seedlings with 200 mM NaCl for 24 h in 0.5 MS medium, the number and fluorescence intensity of P5CS1–GFP dots significantly increased in the root elongation and root hair differentiation zones (Figure 7i,j). In root tips, where P5CS1–GFP showed very low level of expression, some increase in P5CS2–GFP levels was observed upon salt treatment, whereas in the root elongation zone P5CS2–GFP levels were low and apparently unaffected by salt treatment (Figure 7k,l). Immunolocalization of P5CS–GFP proteins in root cross-sections by indirect immunofluorescence detection of anti-GFP antibody using an FITC-labelled second antibody identified the P5CS1–GFP protein only in subcellular bodies within cells of the central cylinder, whereas the P5CS2–GFP protein showed clear cytoplasmic localization in all root cell types (Figure 7m,n). Co-staining of vacuoles with propidium iodide indicated that P5CS1–GFP is not localized in vacuoles, although accumulation of P5CS1–GFP in smaller pro-vacuoles could not be completely excluded (Figure 7m).

In mesophyll cells of intact leaves, P5CS1–GFP and P5CS2–GFP showed similar distribution in both cytoplasm and chloroplasts (Figure 8a,c). Treatment of seedlings with 200 mM NaCl for 24 h led to the re-localization of over 80% of P5CS1–GFP signal into chloroplasts, whereas the fluorescence intensity of cytoplasmic P5CS2–GFP signal was only marginally reduced (i.e. by less then 20%) by the salt treatment (Figure 8b,d). Preparation of leaf mesophyll protoplasts by cell-wall digestion in a medium containing 0.4 M of mannitol resulted in quantitative re-localization of

P5CS1–GFP into chloroplasts, as indicated by the orange colour of overlapping green GFP and chloroplast-derived red fluorescence signals (Figure 8e). By contrast, the chloroplasts were connected with threads of a thin green layer of cytoplasm in optical cross-sections of P5CS2–GFP-expressing protoplasts (Figure 8g). Higher-resolution images through the chloroplast layer confirmed exclusive chloroplast localization of P5CS1–GFP (Figure 8f), whereas orange images of chloroplasts surrounded by a green network of cytoplasm indicated high residual levels of P5CS2–GFP in the cytoplasm (Figure 8h). In conclusion, differential localization of P5CS1–GFP and P5CS2–GFP proteins in various cell types and at the subcellular level supported the genetic data showing that P5CS1 and P5CS2 perform non-overlapping functions.

Discussion

P5CS1 *is required for proline accumulation during osmotic stress*

Many key enzymes in plant metabolic pathways are encoded by duplicated genes, which are thought to perform redundant functions, thus avoiding the possibility of single gene mutations leading to lethal auxotrophy. Gene duplications are often accompanied by sequence alterations causing changes in transcriptional regulation and contributing to evolution of functional divergence (Briggs *et al.*, 2006). The rate-limiting step in proline synthesis is controlled by a bifunctional P5CS enzyme, which is encoded by two highly homologous genes in Arabidopsis and other plants (Fujita *et al.*, 1998; Ginzberg *et al.*, 1998; Strizhov *et al.*, 1997; Yoshiba *et al.*, 1997). Previous studies of Arabidopsis *P5CS* genes revealed significant differences in temporal and spatial regulation of their transcription (Ábrahám *et al.*, 2003; Strizhov *et al.*, 1997). To characterize the extent of functional diversification of *P5CS* genes, we have isolated four *p5cs1* and two *p5cs2* insertion mutant alleles, which all represent recessive loss-of-function mutations. Nonetheless, some *p5cs1* alleles, such as *p5cs1-1* and *p5cs1-3*, represent knockdown rather than knockout mutations, because they carry T-DNA tags in either the 5′ UTR or intron, allowing residual synthesis and maturation of mRNA at 2–6% of the wild-type levels.

Under optimal growth conditions, all *p5cs1* insertion mutants show normal development, although their free proline levels are 15–30% lower in leaves and 35–45% lower in flowers compared to wild-type plants. However, proline synthesis under drought and salt stress is strikingly compromised in the *p5cs1* mutants as they accumulate 3–5 times less proline than the wild-type under stress. Residual stress-stimulated proline accumulation in the *p5cs1* mutants is probably controlled by *P5CS2*, or the ornithine-Δ-aminotransferase (OAT) gene, which are moderately induced by
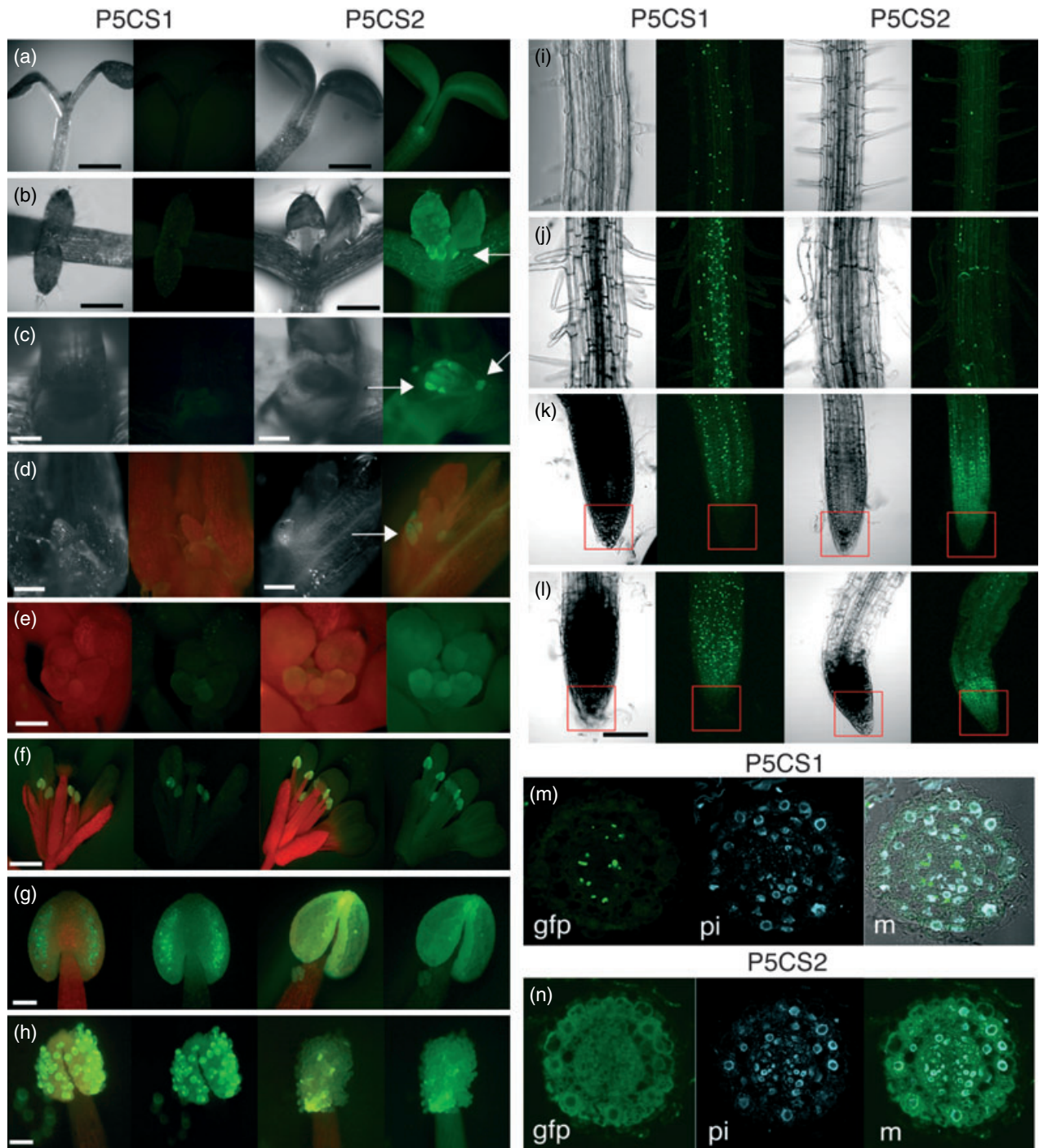
Figure 7. Comparison of spatial expression patterns of P5CS1–GFP and P5CS2–GFP proteins during plant development.

Cotyledons and shoot apical regions of 5-day-old (a) and 8-day-old (b) seedlings (bar = 1 mm). The arrow indicates young leaf primordia.

(c) Apical meristems of 12-day-old seedlings after removal of leaves. P5CS2–GFP marks the positions of leaf primordia (arrows). Bar = 200 μm

(d) Lateral buds of 3-week-old plants. P5CS2–GFP is expressed in leaf primordia and stipules marked by an arrow. Bar = 200 μm.

(e) P5CS1–GFP and P5CS2–GFP expression in inflorescence meristems and flower buds. Bar = 50 μm.

(f) Expression of P5CS–GFP proteins in flowers. Bar = 500 μm.

(g, h) P5CS–GFP patterns in immature (g) and mature (h) anthers and pollen grains. Bars = 50 μm.

(i–l) Localization of P5CS1–GFP and P5CS2–GFP proteins in roots of seedlings incubated in either 0.5 MS medium (control) or 0.5 MS medium containing 150 mM NaCl for 24 h. Bars = 50 μm. P5CS1–GFP and P5CS2–GFP images in elongation zones of control (i) and salt-treated (j) roots, and in root tips marked by red frames of control (k) and salt-stressed (l) roots.

(m, n) Immunohistochemical detection of P5CS1–GFP (m) and P5CS2–GFP (n) in root cross sections. gfp, immunodetection of GFP; pi, staining of vacuoles with propidium iodide; m, merged image.
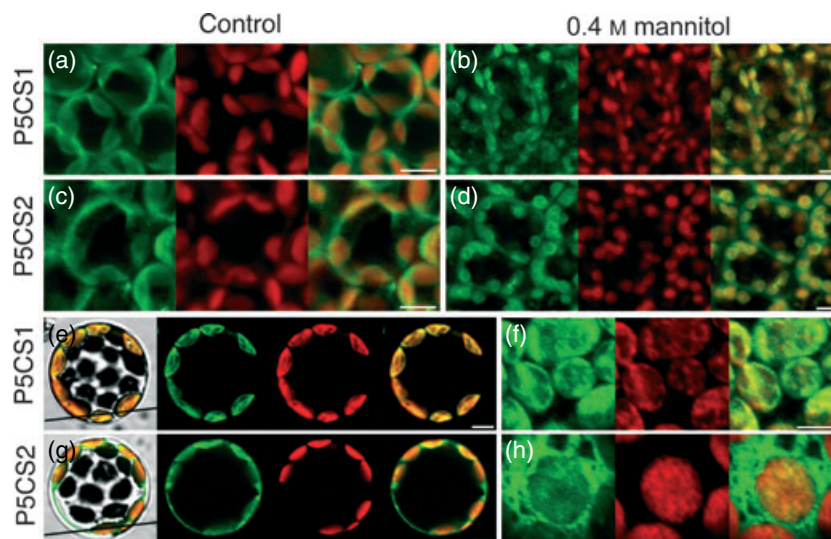
Figure 8. Intracellular localization of P5CS1–GFP and P5CS2–GFP proteins in leaf mesophyll cells (a–d) and leaf mesophyll protoplasts (e–h).
Seedlings were incubated either in water or in 0.4 M mannitol for 4 h and the adaxial leaf surfaces were observed using confocal laser scanning microscopy. GFP (green), chlorophyll autofluorescence (red) and merged images are shown in mesophyll cells of leaves of control P5CS1–GFP (a), mannitol-treated P5CS1–GFP (b), control P5CS2–GFP (c) and mannitol-treated P5CS2–GFP (d) seedlings.
(e–h) Localization of P5CS–GFP proteins in protoplasts prepared from leaves of seedlings described in (a)–(d). The confocal sections were obtained at the mid (e, g) and top surface planes (f,h). From left to right, the photographs show GFP (green), chlorophyll autofluorescence (red) and merged (orange) GFP and chlorophyll images of P5CS1–GFP (e, f) and P5CS2–GFP (g, h) protoplasts. The images on the left are merged bright-field and confocal images, in which black lines indicate the approximate positions of the planes of the confocal sections shown at higher magnification in (f) and (h). Bars = 5 μm.

salt and drought and are similarly expressed in wild-type and *p5cs1* mutant plants (data not shown, Ábrahám *et al.*, 2003; Roosens *et al.*, 1998; Savouré *et al.*, 1995; Strizhov *et al.*, 1997).

Proline has been proposed to act as an osmoprotective molecule (i.e. compatible osmolyte), implicated in the maintenance of redox balance, ROS detoxification, and protection of protein structures through chaperon-like features (Handa *et al.*, 1986; Hong *et al.*, 2000; Kishor *et al.*, 1995; Saradhi *et al.*, 1995). Nevertheless, several recent experiments challenged the assumption that proline accumulation plays a protective role under osmotic stress (Maggio *et al.*, 2002; Mani *et al.*, 2002; Nanjo *et al.*, 2003). In our study, the availability of *p5cs* insertion mutations provided suitable tools to disrupt the rate-limiting step of proline biosynthesis and determine the consequences of proline depletion under osmotic stress. We found that reduced proline accumulation during drought correlates with a limited decrease of relative water content (RWC) in the *p5cs1* mutants. In this respect, the *p5cs1* mutants behave similarly to the low-proline- accumulating Arabidopsis *lwr2* mutant, which shows lower osmotic adjustment and greater water loss during osmotic stress (Verslues and Bray, 2004). Limited reduction of RWC in the *p5cs1* mutants supports the conclusion that proline accumulation is not a major determinant in multi-factorial control of RWC (Handa *et al.*, 1986; Hong *et al.*, 2000; Nanjo *et al.*, 1999).

In comparison to wild-type, the *p5cs1* mutants are also compromised in their capacity to withstand salt stress. The mutants show impaired root elongation, enhanced chlorosis, and ultimate seedling lethality in the presence of 200 mM NaCl. Our results indicate that reduced proline accumulation in the *p5cs1* mutants leads to salt hypersensitivity, not only because of impaired osmotic adjustment but also due to enhanced accumulation of reactive oxygen species (ROS). Enhancement of chlorosis, chlorophyll degradation and lipid peroxidation in salt-stressed *p5cs1* mutants are thus indicative of ROS damage (Alia *et al.*, 2001). ROS are generated by oxidizing metabolic activities in chloroplasts, mitochondria, peroxisomes and microbodies, as well as by membrane-bound NADPH oxidases, cell-wall peroxidases and amine oxidases. On the other hand, ROS toxicity is reduced by a complex metabolic network, which includes scavenging enzymes (e.g. SOD, catalase, ascorbate peroxidase, GST, etc.) and anti-oxidant molecules such as glutathione and ascorbate (Mittler *et al.*, 2004; Møller, 2001). Proline is proposed to protect plant cells from adverse effects of ROS as a singlet oxygen quencher (Alia *et al.*, 2001), reducing free radical levels (Hong *et al.*, 2000; Mehta and Gaur, 1999) and increasing reduced GSH content (Siripornadulsil *et al.*, 2002). Our data suggest that proline may also play a role as an anti-oxidant by reducing lipid peroxidation and through the protection of detoxifying enzymes during stress. APX, GR and GST enzymes are important components of the ROS-scavenging glutathione–ascorbate cycle that controls the removal of O_2^- and H_2O_2 (Mittler *et al.*, 2004). These enzymes show significantly lower activities in the *p5cs1*

mutants compared to wild-type under salt stress, suggesting that proline accumulation is implicated in the control of either the stability or activity of enzymes in the glutathione–ascorbate cycle. The protective effect of proline has been previously described for other enzymes and linked to parallel changes in ubiquitination-dependent proteolysis (Khedr *et al.*, 2003). In correlation with increased ROS production, we detected higher catalase activities in the salt-stressed *p5cs1* mutants compared to wild-type. The fact that *p5cs1* mutants undergo faster salt-induced bleaching and accumulate higher ROS levels than wild-type plants suggests that the observed increase in catalase levels is probably not sufficient to compensate for the lower activity of the detoxifying glutathione–ascorbate cycle. However, it remains to be clarified how these secondary stress responses are affected during progressive drought and salt stress by the reduction of proline levels in the *p5cs1* mutants. Our observation that P5CS1 and P5CS2 are chloroplast-localized enzymes directs particular attention to further study of correlations between defective proline accumulation and ROS generation in chloroplasts of *p5cs1* mutants.

Function of the P5CS2 *gene is essential for embryo and seedling development*

Inhibition of proline biosynthesis by antisense *P5CS1* expression has been reported to cause severe abnormalities in flower development and vascular differentiation (Nanjo *et al.*, 1999). Based on our data, it is now apparent that developmental abnormalities caused by *P5CS1* antisense expression reflect simultaneous inhibition of both *P5CS1* and *P5CS2* genes. In the absence of osmotic stress, all *p5cs1* mutants show normal development of vegetative and generative organs and are fully fertile. On the other hand, *p5cs2* mutations cause abortion of embryos beyond either the torpedo or U-shape stage depending on the humidity levels and growth conditions. The fact that homozygous *p5cs2* mutants rescued by proline feeding still display severe developmental abnormalities indicates that the developmental defects observed previously in antisense *P5CS1* plants were probably caused by partial inhibition of *P5CS2* (Nanjo *et al.*, 1999).

Embryo lethality of *p5cs2* mutants is probably due to proline depletion during the process of seed maturation. This implies that proline transport from maternal tissues into embryos is probably insufficient, and that *P5CS1* cannot compensate for the effect of *p5cs2* mutation in embryos. A gradual build-up of proline deficiency is indicated by delayed development of homozygous *p5cs2* embryos. The chlorophyll deficiency of homozygous *p5cs2* seeds suggests that proline auxotrophy of embryos could result in similar physiological effects to proline limitation during stress, including enhanced ROS formation. ROS accumulation

could ultimately contribute to browning and abortion of embryos. Proline depletion of embryos probably also results in insufficient osmoprotection, as the homozygous *p5cs2* embryos undergo abortion at later developmental stages in a humid environment. Our data demonstrate that embryo lethality of *p5cs2* mutants is not caused by deficiency of *P5CS1* gene expression during embryogenesis. *In situ* hybridization data and *in vivo* analysis of P5CS–GFP expression demonstrate that both *P5CS* genes are transcribed in developing embryos. Surprisingly, we found however that P5CS1–GFP is sequestered into subcellular bodies in embryonic cells. The lethality of *p5cs2* embryos therefore suggests that sequestration of P5CS1 into these so far uncharacterized subcellular bodies leads to proline deficiency in the absence of cytoplasmic P5CS2 enzyme during embryo maturation.

Specification of housekeeping and stress-responsive P5CS functions

Our data show that diversification of P5CS functions in Arabidopsis does not only reflect differences at the level of transcriptional regulation (Ábrahám *et al.*, 2003; Savouré *et al.*, 1995; Strizhov *et al.*, 1997; Yoshiba *et al.*, 1995), but also in cell-type-specific and subcellular localization of P5CS enzymes. Complementation of *p5cs1* and *p5cs2* mutants by the corresponding *P5CS*–GFP gene constructs permitted reliable *in vivo* localization studies with functional GFP-fused enzymes. Intriguingly, we found that P5CS2–GFP expression marks the first leaf primordia in germinating seedlings, and also labels the differentiating leaf primordia and stipules composed of few cells in the apical and auxiliary meristems. As P5CS1–GFP is detected in chloroplasts of fully developed leaves, it is apparent that P5CS2 is expressed much earlier and at higher levels during leaf development than P5CS1. Lack of P5CS2 in leaf primordia of *p5cs2* mutant seedlings could cause slow and aberrant seedling development due to local proline deficiency. Nonetheless, it is rather unexpected that proline transport from P5CS1-expressing tissues cannot compensate for the *p5cs2* deficiency in leaf primordial, and this observation calls for further studies of regulation of proline transport.

Expression patterns of P5CS2–GFP in shoot and root meristems confirm previous data showing that *P5CS2* transcript levels are high in dividing cells (Strizhov *et al.*, 1997). Although P5CS1–GFP and P5CS2–GFP display apparently overlapping expression patterns in roots, P5CS1–GFP also accumulates in subcellular bodies in root cells as in embryos. Moreover, P5CS1–GFP is only expressed in cells of the root cortex, whereas P5CS2–GFP is present in all root cell types and shows cytoplasmic localization. This suggests that subcellular sequestration of P5CS1, which is stimulated by osmotic and salt stress, prevents the compensation of *p5cs2* deficiency not only in embryos but also in roots. In addition,

low expression of P5CS1–GFP in leaf primordia probably also contributes to the lethal phenotype of *p5cs2* mutations. Remarkably, in mesophyll cells of mature leaves, salt and osmotic stress stimulate the import of P5CS1 to chloroplasts, while, in comparison, the distribution of the P5CS2 pool in the cytoplasm and chloroplasts does not show significant change in response to stress. These data suggest that proline biosynthesis from glutamate takes place in both chloroplasts and the cytoplasm of mesophyll cells in leaves, and that import of P5CS1 to chloroplasts contributes to the increase in proline accumulation induced by osmotic stress. In this respect, it is interesting that P5CR, the second enzyme of the glutamate-derived proline bio-synthsis pathway, which is encoded by a single gene in Arabidopsis, is localized both in the cytoplasm and chloro-plast, and its spatial and temporal expression patterns closely resemble that of P5CS2 (Rayapati *et al.*, 1989; Szoke *et al.*, 1992; Verbruggen *et al.*, 1993). By contrast, ornithine aminotransferase and other enzymes of arginine metabo-lism are believed to be mitochondrial (Taylor and Stewart, 1981). Depending on the cell type, it is therefore probable that the glutamate-derived proline biosynthetic pathway is functional both in the cytoplasm and chloroplast. This observation requires further support by confirmatory stud-ies, including the analysis of chloroplast import of P5CS proteins. In addition, detailed understanding of the mecha-nisms involved in cell-type- and tissue-specific regulation of P5CS1 and P5CS2 requires further exploration of cell-type-specific and intracellular control of enzyme activities throughout plant development. Such studies are essential because it is likely that it is not the overall amount, but the critical balance of biosynthesis and degradation, that deter-mines the osmoprotective and developmental functions of proline. Duplicated *P5CS* genes with similar differences in transcriptional regulation have also been reported in other species, including alfalfa (Ginzberg *et al.*, 1998) and tomato (Fujita *et al.*, 1998). Therefore, the results obtained in Arabidopsis have broader implications. In addition, it remains to be seen whether this intriguing mechanism, specifying regulatory interplay between an essential house-keeping gene and its stress-regulated homologue, is unique to the proline biosynthesis pathway or common for other duplicated genes controlling key metabolic steps in plants.

Experimental procedures

Plant material and growth conditions

Plant growth conditions in sterile cultures and controlled growth chambers were as described previously (Koncz *et al.*, 1994). Plant transformation was performed using the *in planta Agrobacterium* infiltration method (Bechtold *et al.*, 1993). Stress treatments were carried out with 3-week-old *in vitro*-cultured plants, which were incubated in 0.5 MS liquid medium containing either 150 or 200 mM NaCl by floating the seedlings with submerged roots on

the surface of 10 ml of medium in 13 cm Petri dishes. Alterna-tively, 6-week-old plants grown in the growth chamber were transferred to hydroponic cultures in plastic boxes filled with Hoagland solution containing NaCl (Hoagland and Arnon, 1938). Gradual drought was imposed on 6-week-old soil-grown plants by withdrawing water for 10 days.

Identification and characterization of p5cs1 *and* p5cs2 *T-DNA insertion mutants*

T-DNA insertion mutants were identified in the SALK (Alonso *et al.*, 2003), GABI-KAT (Rosso *et al.*, 2003) and FLAG (http://dbsgap.versailles.inra.fr/publiclines) databases. Seed samples of T_2 progeny provided by the stock centres were germinated under sterile conditions as described previously (Szabados *et al.*, 2002). PCR screening for insertions was performed using gene-specific primer pairs and combinations of either 5′ or 3′ gene-specific primers with T-DNA end-specific primers (Table S1). Amplified fragments carrying plant DNA/T-DNA insert junctions were iso-lated and subjected to DNA sequencing as described previously (Szabados *et al.*, 2002). The list of junction sequences and structures of T-DNA insertions in the mutant alleles are shown in Appendix S1.

In vitro *culture of immature* p5cs2 *mutant seeds*

Green siliques of *p5cs2-1/+* and *p5cs2-2/+* plants were surface-sterilized and immature seeds were excised under sterile conditions using a stereo microscope. Seeds were cultured in 0.5 MS medium under standard culture conditions (Koncz *et al.*, 1994). Embryos were dissected and prepared for microscopic observation as de-scribed previously (Stangelang and Salehian, 2002). Proline was added to the culture medium at 10 mM final concentration after sterilization. After 4 weeks, developing plants were transferred to fresh medium either with or without proline. Six-week-old plantlets were transferred to soil and either sprayed or watered with 10 mM proline solution.

Histochemical assays of H_2O_2 using 3,3′-diaminobenzidine (DAB)

Detection of H_2O_2 in plant tissues was performed as described previously (Ren *et al.*, 2002). Leaves were detached and placed in a solution containing 1 mg ml^{-1} 3,3′-diaminobenzidine (DAB; Sigma, http://www.sigmaaldrich.com/) and incubated at pH 5.5 for 2 h at room temperature. Leaves were de-stained in hot ethanol (96%) for 10 min, and stored in 96% ethanol. H_2O_2 production was visualized as reddish-brown coloration, which was quantitatively measured using densitometric evaluation (NIH Image software, http://rsb.info.nih.gov/nih-image/).

Measurement of lipid peroxidation, chlorophyll content and free proline

Malondialdehyde (MDA), an end product of lipid peroxidation, was measured using the thiobarbituric acid (TBA) test (Heath and Parker, 1968). Leaf tissue (0.1 g) was homogenized in 0.5 ml of 20% w/v TCA solution. The cell extract was centrifuged at 15 000 ***g*** for 5 min at 4°C, and then 0.5 ml of 1% w/v TBA was added to the supernatant. The mixture was incubated in boiling water for 30 min, and the reaction was stopped on ice. Samples

were cleared by centrifugation at 10 000 *g* for 5 min, and the absorbance of supernatant was measured at 535 and 730 nm. The amount of MDA–TBA complex (appearing as red pigment) was calculated according to the equation: X (%) $= 100 \times (OD_{535} - OD_{730})$. Chlorophyll content was determined according to the method described by Lichtenthaler (1987). Leaf material (0.1 g) was homogenized in liquid nitrogen and treated with 100% acetone for 24 h. The homogenate was centrifuged at 15 000 *g* for 5 min, followed by addition of 80% acetone to the supernatant for 24 h. The optical density was measured using a Shimadzu spectrophotometer at 646.8 and 663.2 nm. The amount of chlorophyll was calculated according to the equations: Chl $a = 12.25\ OD_{663.2} - 2.79\ OD_{646.8}$, Chl $b = 21.5\ OD_{646.8} - 5.1\ OD_{663.2}$ and Chl $a + b = 7.15\ OD_{663.2} + 18.71\ OD_{646.8}$. Free proline content was measured in either leaves or sterile seedlings by colorimetric assay according to the method described by Bates (1973) and modified by Ábrahám *et al.* (2003).

Enzyme assays

Leaf material (1 g) was homogenized at 4°C with 40 mg polyvinyl pyrrolydone (PVP) and 4 ml of 0.1 M phosphate buffer (pH 7.0), containing 0.1 mM EDTA. The homogenates were filtered, and centrifuged at 15 000 *g* for 10 min at 4°C, and the supernatants were used for measurement of enzyme activities. Soluble protein concentration in the supernatant was determined according to the method described by Bradford (1976). Superoxide dismutase (SOD) activity was measured according to the method described by Dhindsa *et al.* (1981). Catalase activity was determined as described by Upadhyaya *et al.* (1985). Glutathione reductase was measured by GSH-mediated 5,5′-dithio-bis(2-nitrobenzoic acid (DTNB) reduction (Smith *et al.*, 1988). Guaiacol peroxidase activity was assayed according to the method described by Hendricks *et al.* (1985). Determination of glutathione-*S*-transferase (GST) activity was performed according to the method described by Habig *et al.* (1974). Ascorbate peroxidase activity was assayed according to the method described by Nakano and Asada (1981). Statistical analyses were performed using the ANOVA program of SigmaStat 3.0 software (http://www.systat.com). Means and standard deviations were calculated from three or more independent experiments. Differences between means were determined using Duncan's multiple range test.

Measurement of water relations

Actual water content (AWC) was expressed using the values obtained from fresh and dry weights of leaves, according to the equation: AWC (%) = $100 \times (FW - DW)/FW$. Dry weight was determined after drying the leaves to a constant weight at 80°C. Relative water content (RWC) was calculated by taking the turgid weight (TW) of plants into account: RWC (%) = $100 \times (FW - DW)/(TW - DW)$. The leaves were imbibed in water for 24 h.

RT-PCR analyses

Transcript levels were monitored by semi-quantitative RT-PCR. Total RNA was isolated from plant tissues using the Tri-reagent method (Chomczynski and Sacchi, 1987). cDNA templates were generated from DNase-treated RNA samples by reverse transcription using SuperScript™ II RNase H⁻ reverse transcriptase (Invitrogen, http://www.invitrogen.com/). PCR reactions were performed in 50 μl volume, using 2 μl cDNA template and Dupla-Taq™ polymerase (Zenon Bio; http://www.zenonbio.hu), using the

following protocol: one cycle of 94°C for 2 min, 20–35 cycles of 94°C for 30 sec, 60°C for 45 sec and 72°C for 1 min. Gene-specific primers p5cs1F and p5cs1R, or p5c1A and p5c1B, were used for detection of *P5CS1* transcripts, while the P2for and P2rev primer pair was employed to amplify P5CS2-specific fragments (Table S1). Primers UBQ10for and UBQ10rev were used for amplification of cDNAs of ubiquitin 10, which served as an internal reference.

In situ *hybridization and indirect immunofluorescence*

Dissected developing seeds were fixed in 4% formalde hyde, embedded in wax, and sectioned (7 μm). Probes for *in situ* hybridization were labelled with digoxigenin-11-UTP. RNA probes were transcribed with T7 and T3 RNA polymerases according to the manufacturer's instructions (Roche Applied Science; http://www.roche-applied-science.com). Probes to detect *P5CS1* and *P5CS2* transcripts were PCR-amplified from cDNA using primer pairs P5C1A-T3 and P5C1B-T7, and P5C2A-T3 and P5C2B-T7, respectively (Table S1). Paraffin was removed from the slides using Histoclear (Fisher Scientific; http://www.fishersci.com), and the sections were rehydrated through an ethanol series followed by proteinase K treatment (1 μg ml⁻¹ in 100 mM Tris-HCl, pH 8.0, 50 mM EDTA, 37°C for 30 min). The slides were rinsed with PBS three times and treated with 0.5% acetic anhydride in 0.1 M triethanolamine (pH 8.0) for 10 min, washed with PBS, and dehydrated through an ethanol series. Hybridization was performed in humidified box in buffer H containing 300 mM NaCl, 10 mM Tris-HCl (pH 6.8), 10 mM Na-phosphate, 5 mM EDTA, 50% formamide, 1× Denhardt's, 10% dextran sulphate, and 1 mg ml⁻¹ tRNA at 50°C. Post-hybridization washes were performed three times in 0.1× SSC for 30 min at 50°C. The hybridized probe–RNA was detected using an anti-DIG-alkaline phosphatase conjugate and the substrates NBT (nitroblue tetrazolium salt) and BCIP (5-bromo-4-chloro-3-indolyl phosphate, toluidinium salt), which give a light-blue precipitate. Microscopic observations were performed using a Zeiss Axioskop 2 microscope (http://www.zeiss.com/). Immunohistochermical localization of P5CS1–GFP and P5CS2–GFP proteins was performed as described previously (Sarnowski *et al.*, 2005). Briefly, root sections were treated with a monoclonal antibody against GFP, followed by detection using an FITC-conjugated secondary antibody. High-resolution images were taken using a Zeiss DSM 940 microscope.

Protein localization

P5CS1–GFP and *P5CS2*–GFP gene constructs were generated by precise replacement of stop codons of *P5CS1* and *P5CS2* genes with coding sequences of the *eGFP* gene (Figure S1). The *P5CS1* genomic DNA was cloned as an *Spe*I fragment (carrying a promoter sequence of 2464 bp), whereas the *P5CS2* gene (including a promoter sequence of 2537 bp) was cloned as an *Xba*I fragment into pBluescript SK vector (Strizhov *et al.*, 1997). The translational stop codons of *P5CS* and *P5CS2* were removed by *in vitro* mutagenesis (Clontech, http://www.clontech.com/), and replaced by *Apa*I restriction sites. The eGFP coding region with its stop codon was cloned into the generated *Apa*I sites, forming in-frame fusions with the *P5CS* genes. The *P5CS1*–GFP and *P5CS2*–GFP gene constructs were cloned into the pPCV812 vector and used for *Agrobacterium*-mediated transformation (Koncz *et al.*, 1994). For GFP localization, leaf mesophyll protoplasts were isolated from P5CS–GFP-expressing transgenic plants according to the methid described by Mathur *et al.* (1995). *In vivo* fluorescence microscopic observations were made using Leica MZFLIII florescence (http://www.

leica-microsystems.com) and Olympus confocal laser scanning microscopes (http://www.olympus.com). For comparison of spatial and temporal expression of GFP reporter constructs, over 20 progeny of at least five independent T_2 families of wild-type, *p5cs1-4* and *p5cs2-1/+* mutants, expressing either P5CS1–GFP or P5CS2–GFP, respectively, were examined. Despite minor variations in expression levels, the expression patterns of P5CS1–GFP or P5CS2–GFP reporters in the independent transgenic lines were identical. Mitochondria were labelled by MitoTracker Orange (Invitrogen; http://www.invitrogen.com).

Computer analysis

For prediction of protein localization, we used the following online services: PSORT (http://psort.nibb.ac.jp/), TargetP (http://www.cbs.dtu.dk/services/TargetP/), Predotar (http://urgi.versailles.inra.fr/tools/predotar/), SubLoc (http://www.bioinfo.tsinghua.edu.cn/SubLoc/), Plant-Ploc (http://chou.med.harvard.edu/bioinf/plant/), Protein Prowler (http://pprowler.imb.uq.edu.au/), and BaCelLo (http://gpcr.biocomp.unibo.it/bacello/pred.htm).

Supplementary Material

The following supplementary materiual is avaiable for this article online:
Figure S1. Structure of the P5CS1–GFP and P5CS2–GFP gene fusions used for protein localization studies.
Table S1. Oligonucleotide primers used in the experiments.
Appendix S1. Map of insertion mutations.
This material is available as part of the online article from http://www.blackwell-synergy.com
Please note: Blackwell Publishing are not responsible for the content or functionality of any supplementary materials supplied by the authors. Any queries (other than missing material) should be directed to the corresponding author for the article.

References

Ábrahám, E., Rigó, G., Székely, G., Nagy, R., Koncz, C. and Szabados, L. (2003) Light-dependent induction of proline biosynthesis by abscisic acid and salt stress is inhibited by brassinosteroid in *Arabidopsis*. *Plant Mol. Biol.* **51**, 363–372.

Alia, P., Mohanty, P. and Matysik, J. (2001) Effect of proline on the production of singlet oxygen. *Amino Acids*, **21**, 195–200.

Alonso, J.M., Stepanova, A.N., Leisse, T.J. *et al.* (2003) Genome-wide insertional mutagenesis of *Arabidopsis thaliana*. *Science*, **301**, 653–657.

Bates, L.S. (1973) Rapid determination of free proline content for water-stress studies. *Plant Soil*, **39**, 205–207.

Bechtold, N., Ellis, J. and Pelletier, G. (1993) *In planta Agrobacterium* mediated gene transfer by infiltration of adult *Arabidopsis thaliana* plants. *C. R. Acad. Sci. III*, **316**, 1194–1199.

Bradford, M.M. (1976) A rapid and sensitive method for the quantitation of microgram quantities of protein utilizing the principle of protein–dye binding. *Anal. Biochem.* **72**, 248–254.

Briggs, G.C., Osmont, K.S., Shindo, C., Sibout, R. and Hardtke, C.S. (2006) Unequal genetic redundancies in Arabidopsis – a neglected phenomenon? *Trends Plant Sci.* **11**, 492–498.

Chomczynski, P. and Sacchi, N. (1987) Single-step method of RNA isolation by acid guanidinium thiocyanate–phenol–chloroform extraction. *Anal. Biochem.* **162**, 156–159.

Csonka, L.N. (1981) Proline overproduction results in enhanced osmotolerance in *Salmonella typhimurium*. *Mol. Gen. Genet.* **182**, 82–86.

Delauney, A. and Verma, D.P.S. (1990) A soybean gene encoding delta 1-pyrroline-5-carboxylate reductase was isolated by functional complementation in *Escherichia coli* and is found to be osmoregulated. *Mol. Gen. Genet.* **221**, 299–305.

Delauney, A. and Verma, D.P.S. (1993) Proline biosynthesis and osmoregulation in plants. *Plant J.* **4**, 215–223.

Deuschle, K., Funck, D., Hellmann, H., Daschner, K., Binder, S. and Frommer, W.B. (2001) A nuclear gene encoding mitochondrial delta-pyrroline-5-carboxylate dehydrogenase and its potential role in protection from proline toxicity. *Plant J.* **27**, 345–356.

Dhindsa, R.S., Plumb-Dhindsa, P. and Thorpe, T.A. (1981) Leaf senescence: correlated with increased levels of membrane permeability and lipid peroxidation, and decreased levels of superoxide dismutase and catalase. *J. Exp. Bot.* **32**, 93–101.

Fabro, G., Kovacs, I., Pavet, V., Szabados, L. and Alvarez, M.E. (2004) Proline accumulation and AtP5CS2 gene activation are induced by plant–pathogen incompatible interactions in *Arabidopsis*. *Mol. Plant Microbe Interact.* **17**, 343–350.

Forlani, G., Scainelli, D. and Nielsen, E. (1997) Δ1-pyrroline-5-carboxylate dehydrogenase from cultured cells of potato: purification and properties. *Plant Physiol.* **113**, 1413–1418.

Fujita, T., Maggio, A., Garcia-Rios, M., Bressan, R.A. and Csonka, L.N. (1998) Comparative analysis of the regulation of expression and structures of two evolutionarily divergent genes for Δ1-pyrroline-5-carboxylate synthetase from tomato. *Plant Physiol.* **118**, 661–674.

Ginzberg, I., Stein, H., Kapulnik, Y., Szabados, L., Strizhov, N., Schell, J., Koncz, C. and Zilberstein, A. (1998) Isolation and characterization of two different cDNAs of Δ1-pyrroline-5-carboxylate synthase in alfalfa, transcriptionally induced upon salt stress. *Plant Mol. Biol.* **38**, 755–764.

Habig, W.H., Pabst, M.J. and Jakoby, W.B. (1974) Glutathione S-transferases. The first enzymatic step in mercapturic acid formation. *J. Biol. Chem.* **246**, 7130–7139.

Handa, S., Handa, A.K., Hasegawa, P.M. and Bressan, R.A. (1986) Proline accumulation and the adaptation of cultured plant cells to water stress. *Plant Physiol.* **80**, 938–945.

Hare, P.D., Cress, W.A. and Van Staden, J. (1999) Proline synthesis and degradation: a model system for elucidating stress-related signal transduction. *J. Exp. Bot.* **50**, 413–434.

Heath, R.L. and Parker, L. (1968) Photoperoxidation in isolated chloroplasts. I. Kinetics and stoichiometry of fatty acid peroxidation. *Arch. Biochem. Biophys.* **125**, 189–198.

Hendricks, T.H., van den Berg, B.M. and Schram, A.W. (1985) Cellular location of peroxidase isoenzymes in leaf tissue of *Petunia* and their affinity for concanavalin A–Sepharose. *Planta*, **164**, 89–95.

Hoagland, D.R. and Arnon, D.I. (1938) *The Water-Culture Method For Growing Plants Without Soil.* Berkeley, CA: University of California College of Agriculture Experimental Station, pp. 347–353.

Hong, Z., Lakkineni, K., Zhang, Z. and Verma, D.P.S. (2000) Removal of feedback inhibition of Δ(1)-pyrroline-5-carboxylate synthetase results in increased proline accumulation and protection of plants from osmotic stress. *Plant Physiol.* **122**, 1129–1136.

Hu, C.A., Delauney, A.J. and Verma, D.P.S. (1992) A bifunctional enzyme (Δ1-pyrroline-5-carboxylate synthetase) catalyzes the first two steps in proline biosynthesis in plants. *Proc. Natl Acad. Sci. USA*, **89**, 9354–9358.

Khedr, A.H., Abbas, M.A., Wahid, A.A.A., Quick, W.P. and Abogadallah, G.M. (2003) Proline induces the expression of salt-stress-responsive proteins and may improve the adaptation of *Pancratium maritimum* L. to salt stress. *J. Exp. Bot.* **54**, 2553–2562.

Kishor, K.P.B., Hong, Z., Miao, G.H.-A., Hu, C.A.-A. and Verma, D.P.S. (1995) Overexpression of [Δ]-pyrroline-5-carboxylate synthetase increases proline production and confers osmotolerance in transgenic plants. *Plant Physiol.* **108**, 1387–1394.

Kiyosue, T., Yoshiba, Y., Yamaguchi-Shinozaki, K. and Shinozaki, K. (1996) A nuclear gene encoding mitochondrial proline dehydrogenase, an enzyme involved in proline metabolism, is upregulated by proline but downregulated by dehydration in *Arabidopsis*. *Plant Cell*, **8**, 1323–1335.

Koncz, C., Martini, N., Szabados, L., Hrouda, M., Bachmair, A. and Schell, J. (1994) Specialized vectors for gene tagging and expression studies. In *Plant Molecular Biology Manual* (Gelvin, S. and Schilperoort, B., eds). Dordrecht, The Netherlands: Kluwer Academic, **B2**, pp. 1–22.

Lichtenthaler, H.K. (1987) Chlorophylls and carotenoids: pigments of photosynthetic biomembranes. *Methods Enzymol.* **148**, 350–382.

Liu, J. and Zhu, J.K. (1997) Proline accumulation and salt-stress-induced gene expression in a salt-hypersensitive mutant of *Arabidopsis*. *Plant Physiol.* **114**, 591–596.

Maggio, A., Miyazaki, S., Veronese, P., Fujita, T., Ibeas, J.I., Damsz, B., Narasimhan, M.L., Hasegawa, P.M., Joly, R.J. and Bressan, R.A. (2002) Does proline accumulation play an active role in stress-induced growth reduction? *Plant J.* **31**, 699–712.

Mani, S., Van De Cotte, B., Van Montagu, M. and Verbruggen, N. (2002) Altered levels of proline dehydrogenase cause hypersensitivity to proline and its analogs in *Arabidopsis*. *Plant Physiol.* **128**, 73–83.

Mathur, J., Koncz, C. and Szabados, L. (1995) A simple method for isolation, liquid culture, transformation and regeneration of *Arabidopsis thaliana* protoplasts. *Plant Cell Rep.* **14**, 221–226.

Mehta, S.K. and Gaur, J.P. (1999) Heavy-metal-induced proline accumulation and its role in ameliorating metal toxicity in *Chlorella vulgaris*. *New Phytol.* **143**, 253–259.

Mittler, R., Vanderauwera, S., Gollery, M. and Van Breusegem, F. (2004) Reactive oxygen network of plants. *Trends Plant Sci.* **9**, 490–498.

Møller, I.M. (2001) Plant mitochondria and oxidative stress: electron transport, NADPH turnover, and metabolism of reactive oxygen species. *Annu. Rev. Plant Physiol. Plant Mol. Biol.* **52**, 561–591.

Nakano, Y. and Asada, K. (1981) Hydrogen peroxide is scavenged by ascorbate-specific peroxidase in spinach chloroplasts. *Plant Cell Physiol.* **22**, 867–880.

Nanjo, T., Kobayashi, M., Yoshiba, Y., Sanada, Y., Wada, K., Tsukaya, H., Kakubari, Y., Yamaguchi-Shinozaki, K. and Shinozaki, K. (1999) Biological functions of proline in morphogenesis and osmotolerance revealed in antisense transgenic *Arabidopsis thaliana*. *Plant J.* **18**, 185–193.

Nanjo, T., Fujita, M., Seki, M., Kato, T., Tabata, S. and Shinozaki, K. (2003) Toxicity of free proline revealed in an *Arabidopsis* T-DNA-tagged mutant deficient in proline dehydrogenase. *Plant Cell Physiol.* **44**, 541–548.

Peng, Z., Lu, Q. and Verma, D.P.S. (1996) Reciprocal regulation of Δ1-pyrroline-5-carboxylate synthetase and proline dehydrogenase genes controls proline levels during and after osmotic stress in plants. *Mol. Gen. Genet.* **253**, 334–341.

Rayapati, P.J., Stewart, C.R. and Hack, E. (1989) Pyrroline-5-carboxylate reductase in pea (*Pisum sativum* L.) leaf chloroplasts. *Plant Physiol.* **91**, 581–586.

Ren, D., Yang, H. and Zhang, S. (2002) Cell death mediated by MAPK is associated with hydrogen peroxide production in *Arabidopsis*. *J. Biol. Chem.* **277**, 559–565.

Roosens, N.H., Thu, T.T., Iskandar, H.M. and Jacobs, M. (1998) Isolation of the ornithine-delta-aminotransferase cDNA and effect of salt stress on its expression in *Arabidopsis thaliana*. *Plant Physiol.* **117**, 263–271.

Rosso, M.G., Li, Y., Strizhov, N., Reiss, B., Dekker, K. and Weisshaar, B. (2003) An *Arabidopsis thaliana* T-DNA mutagenized population (GABI-Kat) for flanking sequence tag-based reverse genetics. *Plant Mol. Biol.* **53**, 247–259.

Saradhi, P., Alia, P., Arora, S. and Prasad, K.V. (1995) Proline accumulates in plants exposed to UV radiation and protects them against UV induced peroxidation. *Biochem. Biophys. Res. Commun.* **209**, 1–5.

Sarnowski, T.J., Rios, G., Jasik, J. et al. (2005) SWI3 subunits of putative SWI/SNF chromatin-remodeling complexes play distinct roles during Arabidopsis development. *Plant Cell*, **17**, 2454–2472.

Savouré, A., Jaoua, S., Hua, X.J., Ardiles, W., Van Montagu, M. and Verbruggen, N. (1995) Isolation, characterization, and chromosomal location of a gene encoding the Δ1-pyrroline-5-carboxylate synthetase in *Arabidopsis thaliana*. *FEBS Lett.* **372**, 13–19.

Siripornadulsil, S., Traina, S., Verma, D.P.S. and Sayre, R.T. (2002) Molecular mechanisms of proline-mediated tolerance to toxic heavy metals in transgenic microalgae. *Plant Cell*, **14**, 2837–2847.

Smith, I.K., Vierheller, T.L. and Thorne, C.A. (1988) Assay of glutathione reductase in crude tissue homogenates using 5,5'-dithiobis(2-nitrobenzoic acid). *Anal. Biochem.* **175**, 408–413.

Stangelang, B. and Salehian, Z. (2002) An improved clearing method for GUS assay in *Arabidopsis* endosperm and seeds. *Plant Mol. Biol. Rep.* **20**, 107–114.

Strizhov, N., Ábrahám, E., Ökrész, L., Blickling, S., Zilberstein, A., Schell, J., Koncz, C. and Szabados, L. (1997) Differential expression of two *P5CS* genes controlling proline accumulation during salt-stress requires ABA and is regulated by ABA1, ABI1 and AXR2 in *Arabidopsis*. *Plant J.* **12**, 557–569.

Szabados, L., Kovács, I., Oberschall, A. et al. (2002) Distribution of 1000 sequenced T-DNA tags in the *Arabidopsis* genome. *Plant J.* **32**, 233–242.

Szoke, A., Miao, G.H., Hong, Z. and Verma, D.P.S. (1992) Subcellular location of Δ-pyrroline-5-carboxylate reductase in root/nodule and leaf of soybean. *Plant Physiol.* **99**, 1642–1649.

Taylor, A. and Stewart, G. (1981) Tissue and subcellular localization of enzymes of arginine metabolism in *Pisum sativum*. *Biochem. Biophys. Res. Commun.* **101**, 1281–1289.

Upadhyaya, A., Sankhla, D., Davis, T.D., Sankhla, N. and Smith, B.N. (1985) Effect of paclobutrazol on the activities of some enzymes of activated oxygen metabolism and lipid peroxidation in senescing soybean leaves. *J. Plant Physiol.* **121**, 453–461.

Verbruggen, N., Villarroel, R. and Van Montagu, M. (1993) Osmoregulation of a pyrroline-5-carboxylate reductase gene in *Arabidopsis thaliana*. *Plant Physiol.* **103**, 771–781.

Verbruggen, N., Hua, X.J., May, M. and Van Montagu, M. (1996) Environmental and developmental signals modulate proline homeostasis: evidence for a negative transcriptional regulator. *Proc. Natl Acad. Sci. USA*, **93**, 8787–8791.

Verslues, P.E. and Bray, E.A. (2004) LWR1 and LWR2 are required for osmoregulation and osmotic adjustment in *Arabidopsis*. *Plant Physiol.* **136**, 2831–2842.

Yoshiba, Y., Kiyosue, T., Katagiri, T., Ueda, H., Mizoguchi, T., Yamaguchi-Shinozaki, K., Wada, K., Harada, Y. and Shinozaki, K. (1995) Correlation between the induction of a gene for

Δ1-pyrroline-5-carboxylate synthetase and the accumulation of proline in *Arabidopsis thaliana* under osmotic stress. *Plant J.* **7**, 751–760.

Yoshiba, Y., Kiyosue, T., Nakashima, K., Yamaguchi-Shinozaki, K. and Shinozaki, K. (1997) Regulation of levels of proline as an osmolyte in plants under water stress. *Plant Cell Physiol.* **38**, 1095–1102.

Zhang, C.S., Lu, Q. and Verma, D.P.S. (1995) Removal of feedback inhibition of Δ1-pyrroline-5-carboxylate synthetase, a bifunctional enzyme catalyzing the first two steps of proline biosynthesis in plants. *J. Biol. Chem.* **270**, 20491–20496.